Electronic Supplementary Material (ESI) for Nanoscale.

Supported Information

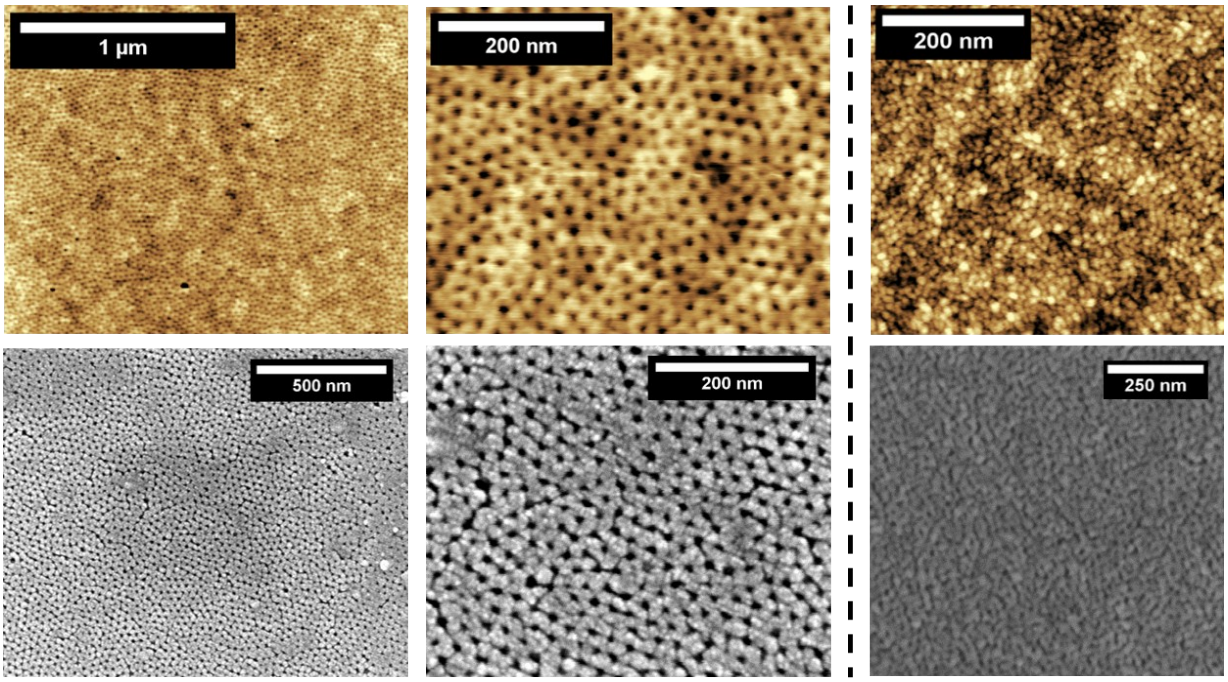

Figure S1: AFM (top) and SEM (bottom) images of PIB_{50}-*b*-PEO_{45} (left and mid column) and Pluronic® F127 (right column) templated mesoporous TiO_2 thin film prepared via spin-coating at different magnifications.

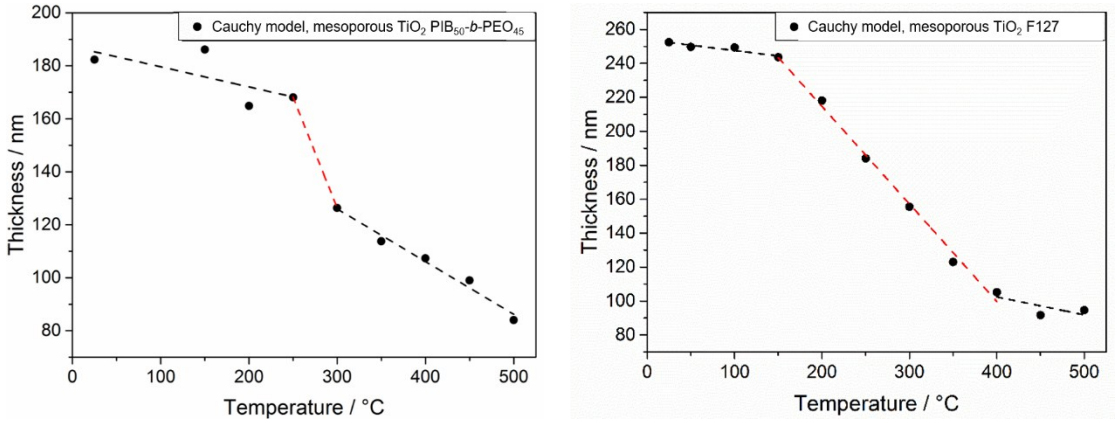

Figure S2: Thickness of the TiO_2 thin films prepared using PIB_{50}-*b*-PEO_{45} (left) and Pluronic® F127 (right) in dependence of the heating temperature provided by spectral ellipsometry. Three different linear fits were utilized to calculate the thickness every 5 °C and are also shown. The dashed red line indicates the temperature range of the decomposition of the block copolymer.

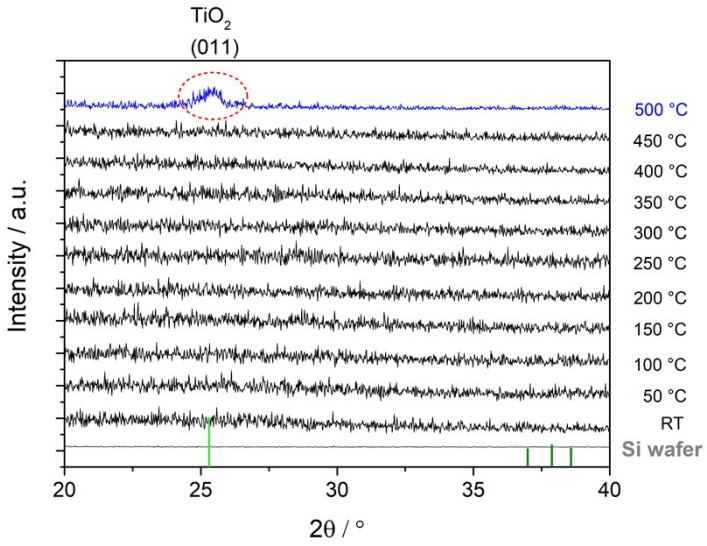

Figure S3: X-ray diffraction patterns of the anatase thin films via spin-coating after heat treatment at different temperatures ranging from room temperature to 500 °C. In addition, the utilized silicon wafer and the anatase reference pattern (ICDS 98-015-4604) are shown. The operating method was 2θ – mode with an incident angle of 1°.

Table S1: Assignments of the most prominent bands of the FTIR investigations of the mesoporous TiO_2 thin films during the intrinsic in-plane stress analyses.

Wavenumber / cm^{-1}	Vibration mode	Origin
3328	ν(O-H)	EtOH, dest. H_2O, PIB_{50}-*b*-PEO_{45}
2956	ν(C-H)	$Ti(O^iPr)_4$, EtOH, PIB_{50}-*b*-PEO_{45}
1636	ν(C=C)	PIB_{50}-*b*-PEO_{45}
1079	ν(C-O)	$Ti(O^iPr_4)$, PIB_{50}-*b*-PEO_{45}
819	δ(=CH), out-of-plane	PIB_{50}-*b*-PEO_{45}
677	ν(Ti-O)[58]	TiO_2 (anatase)
435	ν(Ti-O-Ti)[58]	TiO_2 (anatase)

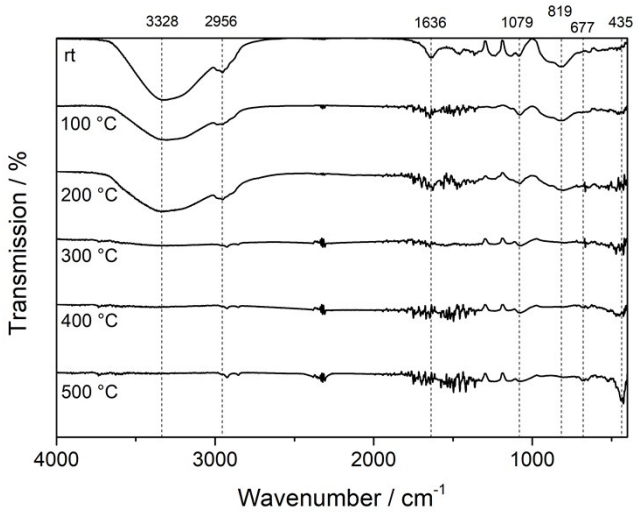

Figure S4: FTIR measurements of the mesoporous TiO_2 thin films after deposition (rt) and heating them to 100 °C, 200 °C, …500 °C analogously to the intrinsic measurement. The prominent peaks are depicted with the corresponding wavenumber and are explained in Table S1.

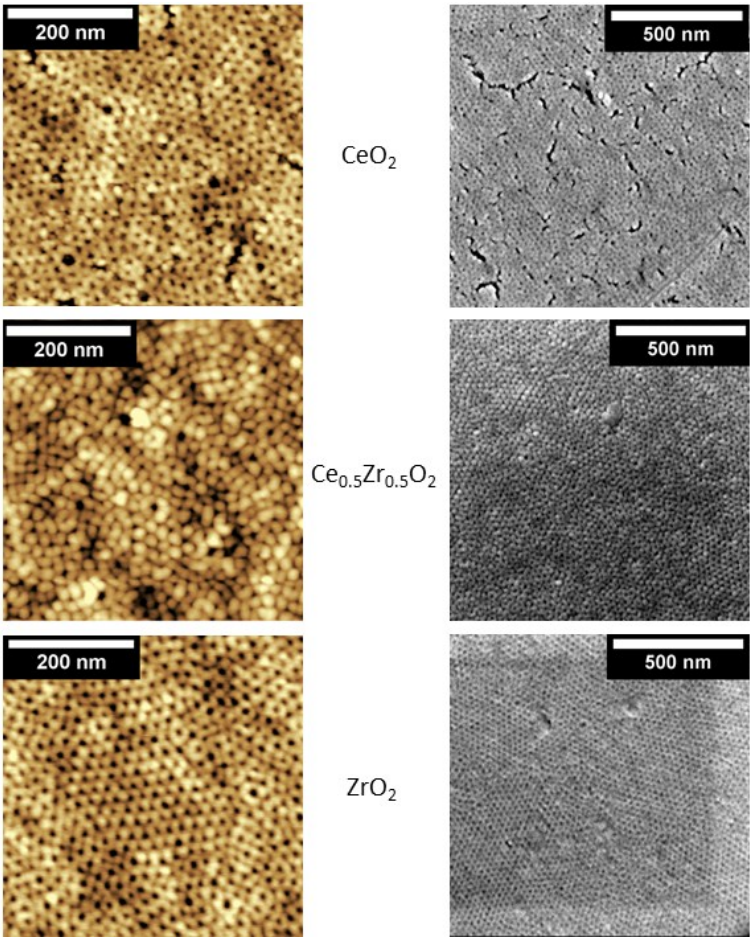

Figure S5: AFM (left) and SEM (right) pictures of the mesoporous CeO_2, CZO and ZrO_2 thin films after the heat treatment at 300 °C.

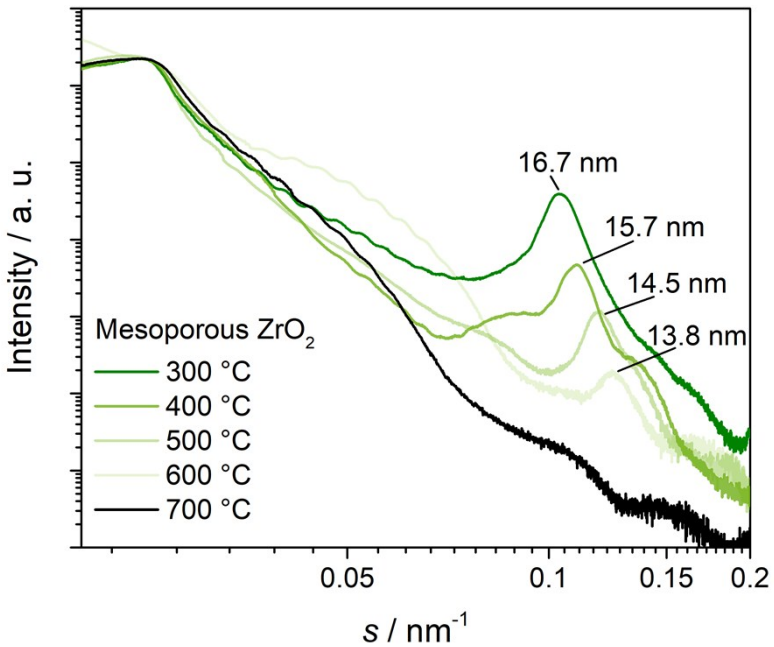

Figure S6: GI-SAXS investigations of the mesoporous ZrO_2 thin films in dependence of the temperature ranging from 300 °C till 1000 °C. Additionally, the calculated pore-to-pore distance is depicted.

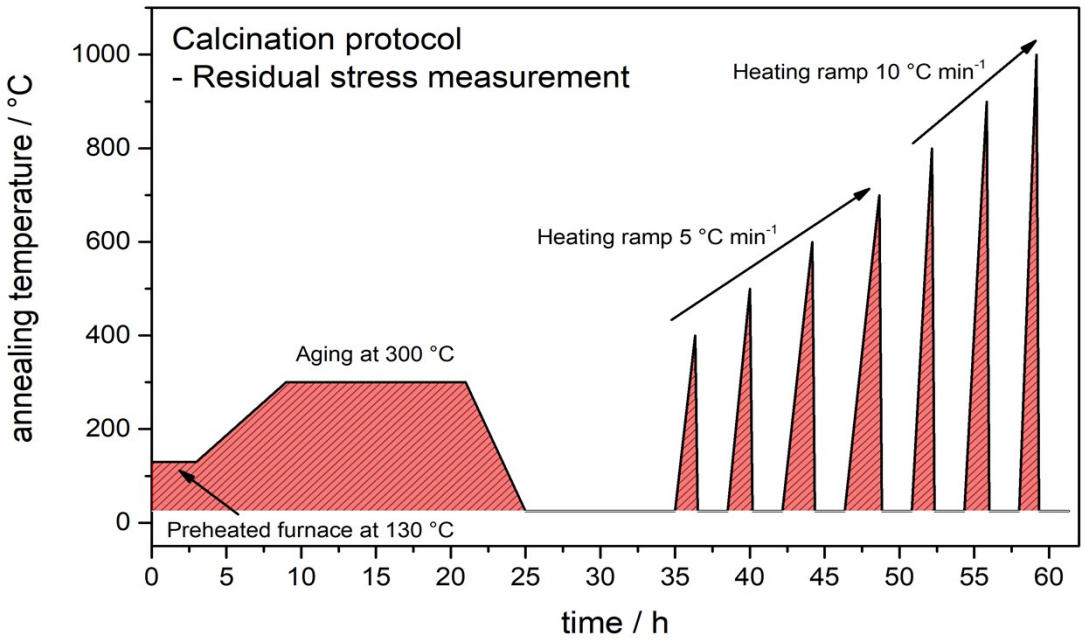

Figure S7: Calcination protocol of the mesoporous thin films used for the residual stress measurement. After the samples were cooled down under ambient air, the residual stress was investigated and subsequently annealed to higher temperature.

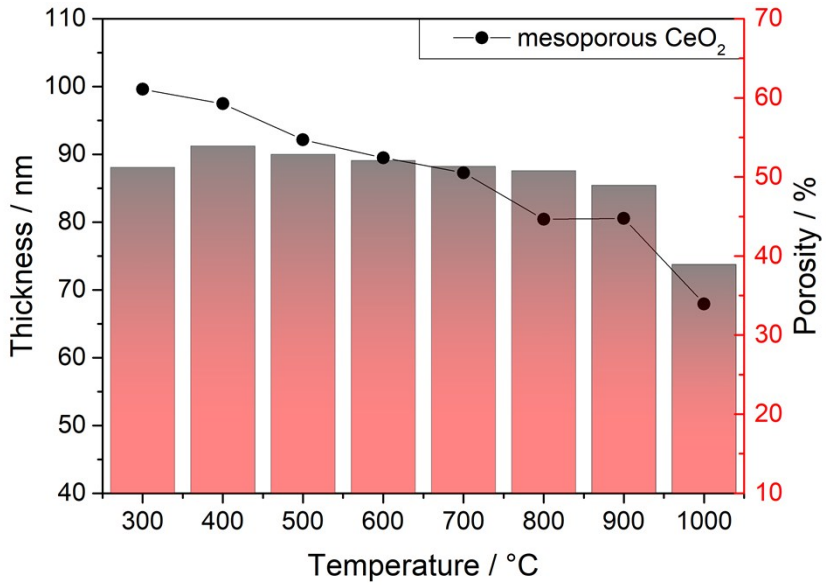

Figure S8: Thickness (circles) and porosity (pillar) of mesoporous CeO_2 thin film in dependence of the heating temperature. The porosity was calculated via Equation (3).

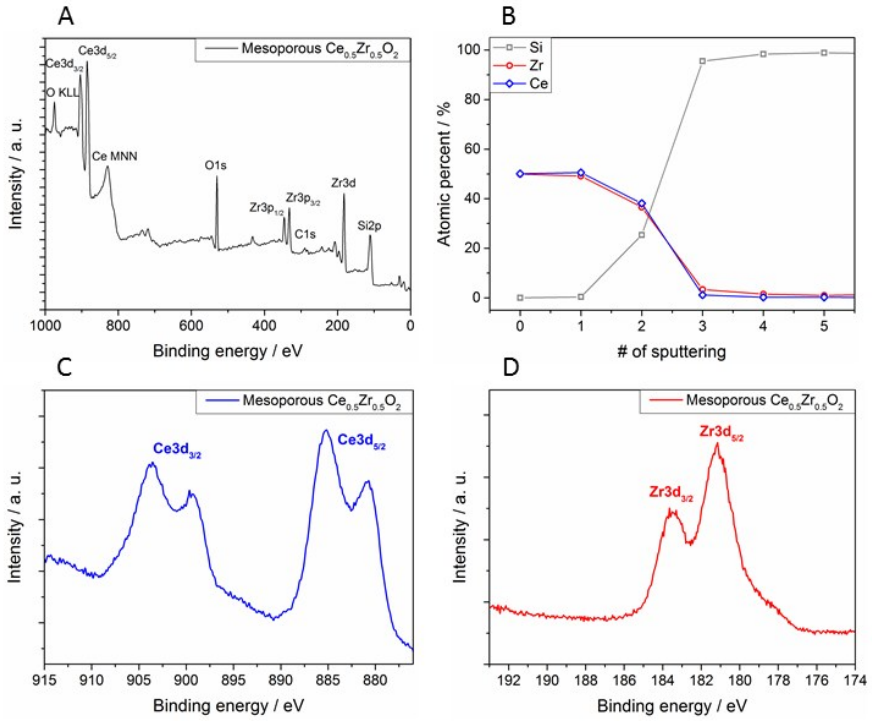

Figure S9: XPS results of the CZO thin films verifying a 50:50-composite. Next to a wide scan to detect all the relevant peaks (A), a detailed narrow scan of the Ce3d (C) and Zr3d (D) was performed. Here, a Shirley background together with Lorentz-Gaussian plots was applied to integrate the peaks and calculate the Ce/Zr-ratio. The determination was executed after every sputter step to create a depth profile (B).

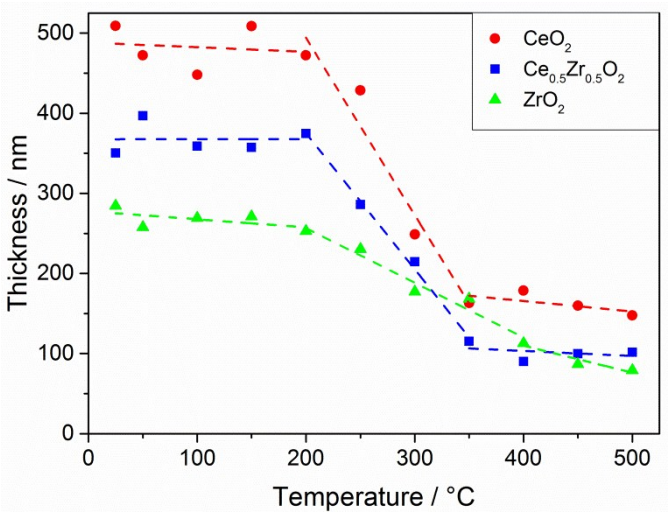

Figure S10: Thickness of the mesoporous CeO_2, CZO and ZrO_2 thin films prepared using PIB_{50}-*b*-PEO_{45} in dependence of the heating temperature provided by spectral ellipsometry. Three different linear fits were utilized to calculate the thickness every 5 °C and are also shown.

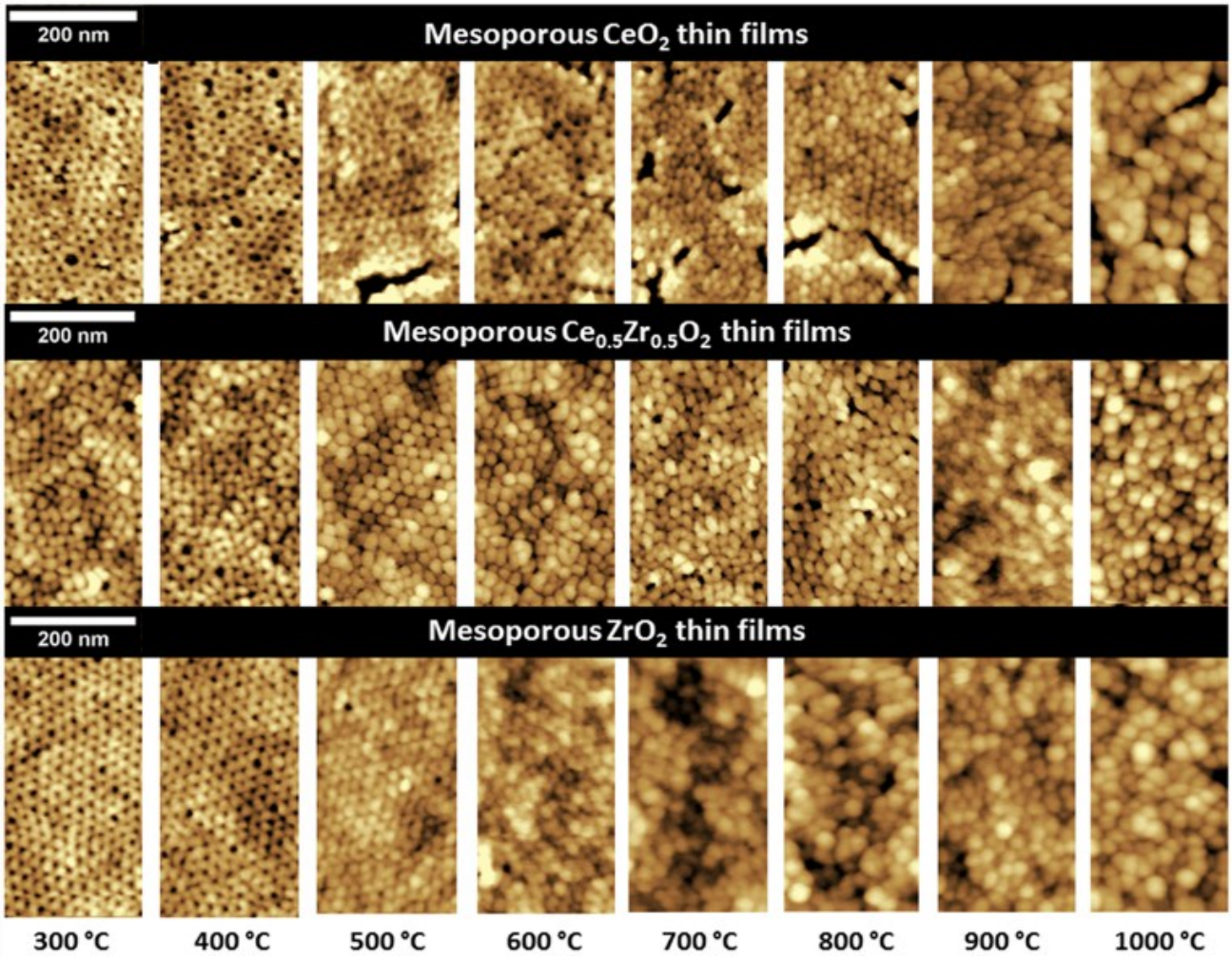

Figure S11: AFM images employing dynamic mode of the mesoporous CeO_2, $Ce_{0.5}Zr_{0.5}O_2$ and ZrO_2 thin films in dependence of the temperature ranging from 300 °C to 1000 °C.